PHILOSOPHICAL TRANSACTIONS OF THE ROYAL SOCIETY A MATHEMATICAL, PHYSICAL & ENGINEERING SCIENCES

Flare Energy Release: Observational Consequences and Signatures [and Discussion]

Richard C. Canfield, J.-F. De La Beaujardiere, K. D. Leka, E. R. Priest, R. C. Canfield and J. C. Henoux

Phil. Trans. R. Soc. Lond. A 1991 **336**, 381-388
doi: 10.1098/rsta.1991.0088

Flare energy release: observational consequences and signatures

By Richard C. Canfield, J.-F. de La Beaujardiere and K. D. Leka

Institute for Astronomy, University of Hawaii, 2680 Woodlawn Drive, Honolulu, Hawaii 96822, U.S.A.

It is generally accepted, but not yet compellingly demonstrated, that the energy released in solar flares is stored in stressed magnetic fields. Little is known, at present, about how the most obvious manifestations of flare energy release – heating, mass motion, magnetic field reconfiguration and particle acceleration – are related to the spatial distribution of free energy within those fields. To address this issue we have underway at Mees Solar Observatory a programme of simultaneous polarimetric and spectroscopic observations that allow us to explore the spatial relation between active region currents, flare particle acceleration and flare heating. In this paper we discuss several days observations of two flare-productive active regions. By using the Haleakala Stokes polarimeter, we observed the spatial distribution of the Stokes profiles of two photospheric Fe^{I} lines, from which we inferred the spatial distribution of the vector magnetic field and the vertical current density. In flares that were observed on the same days, we then compared the locations of vertical currents to the sites of non-thermal electron precipitation and high coronal pressure inferred from Hα line profiles and spectroheliograms obtained with the Mees charge coupled device imaging spectrograph. Without exception we found that the sites of significant energetic electron precipitation into the chromosphere were at the edges of regions of vertical current, not within them. In contrast, we found that the footpoints of high-pressure flare plasmas during the main phase of the observed flares all coincided very well with such currents.

1. Introduction

In this paper we will concentrate on an aspect of energy release in solar flares that will certainly receive considerable attention during this solar cycle, owing to the X-ray imaging capabilities of the *Solar-A* hard X-ray telescope (HXT) and soft X-ray telescope (SXT), combined with improvements in the optical polarimeters with which vector magnetic field data is obtained. The pioneering work relating vector magnetic fields and currents to solar flares was done in the 1960s in the Soviet Union (see, for example, Moreton & Severny 1968). More recently, important contributions have come from Canada, China and the United States (see, for example, Lin & Gaizauskas 1987; Ding *et al.* 1987; Hagyard 1988). These authors clearly showed that there exists a close morphological relation between sites of vertical electrical currents in the photosphere (inferred from vector magnetograms) and sites of solar flares seen in Hα. To our way of thinking, this is the most compelling evidence available, at present, that solar flares are powered by the free magnetic energy stored in non-

Phil. Trans. R. Soc. Lond. A (1991) **336**, 381–388
Printed in Great Britain

potential fields. In the present paper we carry such work one step further, and address the relation of active region currents to specific manifestations of flare energy release, specifically heating and non-thermal electron acceleration.

2. Magnetic fields and current systems

NOAA active regions (AR) 5747 (October 1989) and 6233 (August 1990) clearly showed non-potential photospheric magnetic field structures and produced many flares, several of which we observed at Mees Solar Observatory. By using the Haleakala Stokes polarimeter (Mickey 1975), we obtained daily vector magnetograms for each of five successive days from 18 to 22 October 1989 and each of four successive days from 28 to 31 August 1990. The polarimeter scans are made with a circular aperture of 6 arcsec diameter; the October 1989 data are sampled each 5.7 arcsec, the August 1990 data each 2.8 arcsec (critically sampled). For our inversion of the observed Stokes profiles of the Fe^{I} λ6301.5 and λ6302.5 lines we used the computer code of Lites & Skumanich (1987), which determines the photospheric magnetic and thermodynamic parameters that give the best least-squares fit of theoretical analytical Stokes profiles to the data. We used that code to analyse both Fe^{I} lines simultaneously and to make a first-order correction for unresolved magnetic-field structure. To resolve the 180° ambiguity we followed a multi-step procedure in which our first approximation was to adopt the choice of directions closest to that of the potential field fitted to the line of sight component of the observed magnetic field (Sakurai *et al.* 1985). This procedure works well at most points, but it fails in the most interesting regions. In strongly non-potential regions (e.g. departures of more than 45° from the azimuth of the potential field) we took into account the requirement of continuous change of direction between adjacent pixels (Aly 1989). If ambiguity still existed we chose the direction that minimized the amplitude and small-scale variation of the vertical current density implied by $\nabla \times \boldsymbol{B}$. As well, we chose the direction that minimized vertical currents in regions of horizontal fields (e.g. inversion lines in the line of sight field). Finally, we used the Hα fibrils and filaments shown in movies from Big Bear Solar Observatory to help establish larger scale connectivity. Figure 1 shows the resulting ambiguity-resolved vector magnetogram for 20 October 1989, overlaid on a sunspot image. Flare sites were located in the southern spot complex, along the vertical-field inversion line, where strong observed shear and large field strength obtained for more than 10^4 km along the inversion line, in agreement with the criteria for flare occurrence established by the group at MSFC (Moore *et al.* 1987).

3. Signatures of chromospheric energy release

The response of the Hα line of hydrogen to several energy release processes is relatively well understood. Through numerical modelling of flare chromospheres under the influence of heating by non-thermal electrons, thermal conduction from the overlying corona and coronal pressure, Canfield *et al.* (1984) determined two unique signatures. First, only high values of the energy flux of non-thermal electrons

PHILOSOPHICAL TRANSACTIONS OF THE ROYAL SOCIETY A MATHEMATICAL, PHYSICAL & ENGINEERING SCIENCES

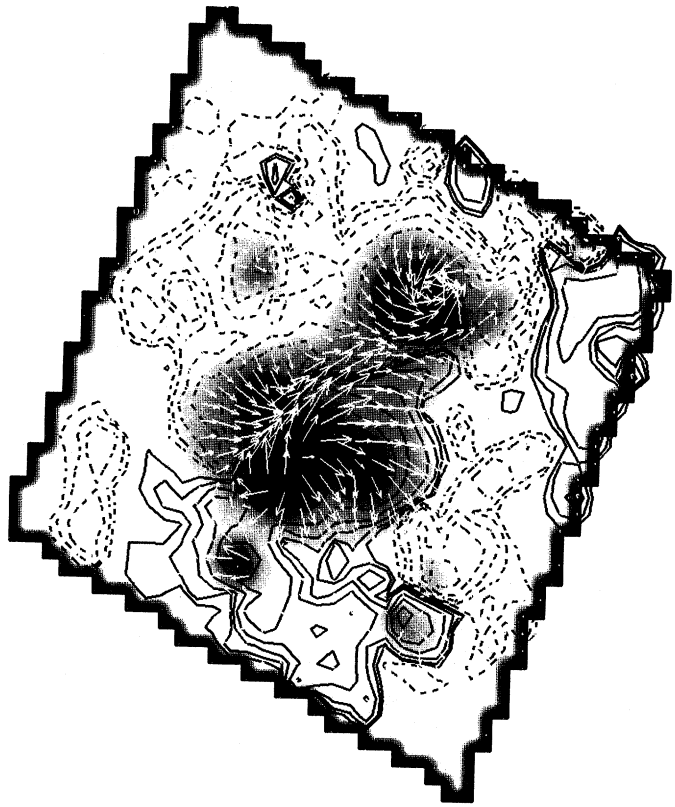

Figure 1. The Mees Solar Observatory ambiguity-resolved vector magnetogram of 20 October 1989, scanned from 17:41 to 18:33UT, transformed from image-plane to heliographic coordinates (North is up, East to the left here and below). The gray-scale image shows the sunspot structure of the active region seen in the continuum near the λ6302.5 line. The contours indicate the vertical magnetic field distribution averaged over each pixel. Radial field contours are shown at 25×2^n gauss levels ($n = 0, 1, \ldots$; dashed contours indicate negative fields) here and below. The arrows show the strength and direction of the transverse field; a length equal to the sampling interval represents a transverse field of strength *ca.* 700 gauss. (1 gauss = 10^{-4} T.)

(greater than 10^{10} erg cm^{-2} s^{-1}† above 20 keV in their models) combined with low coronal pressure (less than 100 dyn cm^{-2}‡) produce Hα profiles that are centrally reversed yet have broad wings that extended beyond 3 Å§ from line centre. Second, only high values of coronal pressure (greater than 1000 dyn cm^{-2}) produce emission profiles that are not centrally reversed. We can therefore search for these signatures in observed flare line profiles, and thereby identify sites of non-thermal electron precipitation and high coronal pressure.

Using the Mees charge coupled device (MCCD) imaging spectrograph (Penn *et al.* 1991) we obtained the four-dimensional flare intensity I (x, y, λ, t) that can be displayed as Hα line profile and/or spectroheliogram time series. MCCD datasets were obtained throughout the following flares: 1N/C5 at 21:34UT, 20 October 1989; SN/C5 at 20:05UT, 21 October 1989; 2B/X3 at 18:05UT, 22 October 1989; 1N/M1.6 at 20:35UT, 29 August 1990. Observed Hα line profiles from the flare of 20

† 1 erg = 10^{-7} J. ‡ 1 dyn = 10^{-5} N. § 1 Å = 10^{-10} m = 10^{-1} nm.

PHILOSOPHICAL TRANSACTIONS OF THE ROYAL SOCIETY A MATHEMATICAL, PHYSICAL & ENGINEERING SCIENCES

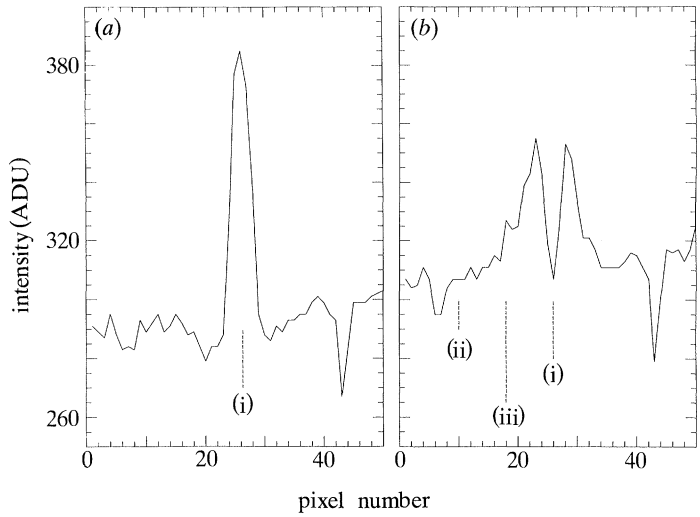

Figure 2. Examples of Hα spectra from the 20 October 1989 flare showing the signatures of intense non-thermal electron precipitation (*a*) broad emission profile with a strong central reversal) and high coronal pressure (*b*) narrow emission profile without a central reversal). The horizontal axis shows the CCD pixel number in the direction parallel to the spectral dispersion, and the 50 pixels cover approximately 20 Å. The vertical axis shows specific intensity in arbitrary units. All but the weakest absorption features are photospheric and telluric lines. (i) Line centre; (ii) continuum; (iii) 2.5 Å blue wing.

October 1989 are shown in figure 2. It is obvious by inspection of the figure that the unreversed, narrow profile on the left (identified with high coronal pressure) lacks the central reversal and broad wings (identified with intense non-thermal electron precipitation in a low-pressure corona) that characterize the profile on the right. The profiles shown are neither cospatial nor cotemporal; the broad self-reversed profile was observed about five minutes before flare maximum, when the unreversed profile was obtained.

4. Morphology of currents and energy release

To determine the spatial relation between sites of vertical current, flare non-thermal electron precipitation, and high coronal pressure, we co-register the vector magnetograms and Hα spectroheliograms using sunspot structures. Both the Stokes polarimeter and the CCD imaging spectrograph record spectra that extend to the continuum near the lines observed; from the polarimeter scan we make a map in the continuum near λ6302.5; from the MCCD datacube we make a spectroheliogram in the continuum near Hα. These images contain many sunspot features that we can use to co-register these two images in a least-squares best-fit sense. The residuals of the fit indicate that the co-registration of each individual spectroheliogram with the vector magnetogram is good to better than 2.9 arcsec, i.e. about half a magnetogram pixel.

(*a*) *Active region 5747*

The current system of this active region is relatively simple throughout the five days of our observations. The two primary upward current sites and one main downward site can be seen in figure 3, which shows the current and magnetic field

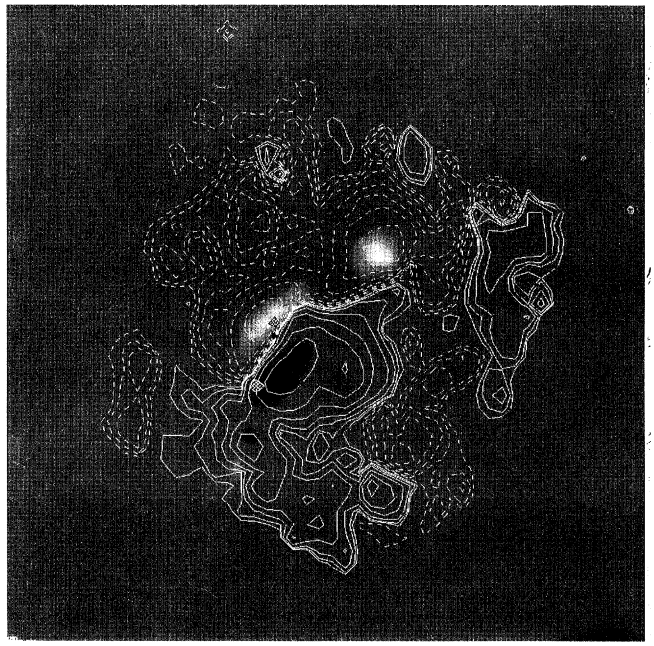

Figure 3. Heliographic map of vertical current density (grey scale), vertical magnetic field (contours), and sites of the Hα signatures of non-thermal electron precipitation (solid black) and high coronal pressure (cross-hatched black and white), in AR 5247 and the flare of 21:34UT on 20 October 1989. The image orientation and vertical field contours are the same as figure 1. Positive currents are shown in white, negative in black. The terrestrial East–West dimension of the vector magnetogram is approximately 140 Mm.

maps for 20 October 1989. We assume that the observed currents close within the scanned field of this magnetogram, since other magnetograms with larger fields of view show no other regions of substantial field. The fact that positive and negative currents balance to *ca.* 1% of the computed total current supports this assumption. Simply from current balance arguments it is clear that two large-scale vertical currents, which we call the eastern and western currents, flow through the photosphere into the corona. Both currents enter the photosphere from the corona in the single large negative current site. The eastern current spans the most highly non-potential section of the polarity inversion line; its southern intersection with the photosphere is very close to that of the western current.

In all three flares that we observed in this active region we found that the sites of non-thermal electron precipitation bore a much different morphological relation to the currents than the sites of high coronal pressure. To within the resolution afforded by the 2.2 arcsec pixels of the MCCD imaging spectrograph observations, only a single precipitation site was found in all events. These were all located at the edges of sites of vertical currents, not within them. In contrast, sites of high coronal pressure, without exception, were located within sites of vertical current, not at their edges. As an example, figure 3 shows the flare of 20 October. The site of particle precipitation is located essentially on the vertical field inversion line, to within the spatial resolution afforded by the 5.7 arcsec pixels.

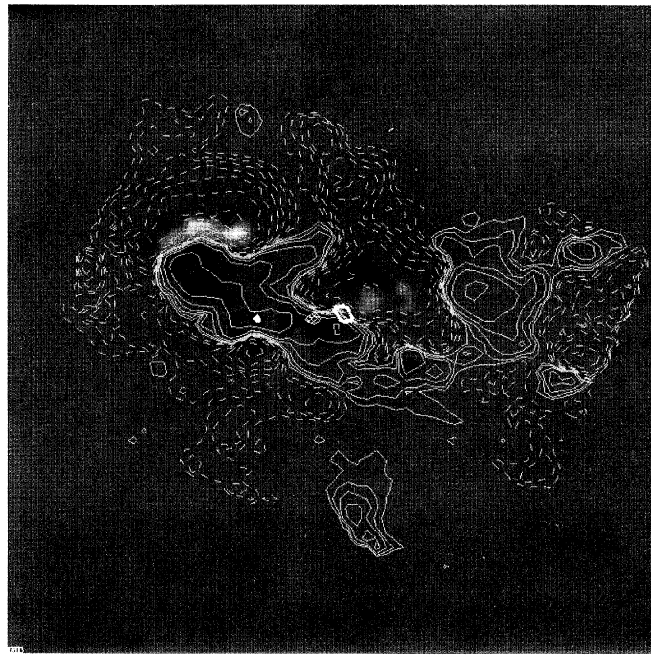

Figure 4. Heliographic map of vertical current density (grey scale), vertical magnetic field (contours), and sites of the Hα signatures of non-thermal electron precipitation (white and white-encircled) and high coronal pressure (white cross-hatched) in NOAA AR6233 and the flare of 20:35UT on 29 August 1990. The image orientation, current, and field conventions are the same as figure 3. The terrestrial East–West dimension of the magnetogram is approximately 114 Mm.

(*b*) *Active region 6233*

The distribution of vertical currents of this active region, shown in figure 4, is more complex than AR 5247. This is only partly due to the better resolution of the vector magnetogram, which is critically sampled twice per 6 arcsec aperture. Again, it is reasonable to assume that the observed currents close within the scanned field of the magnetogram, since positive and negative currents again balance to *ca.* 1%. The greater complexity of these sites precludes a simple speculation on how these sites are connected.

In this flare we again found that the sites of non-thermal electron precipitation bear a much different morphological relation to the currents than the sites of high coronal pressure. In this flare two precipitation sites were found, although it must be noted that the precipitation signature was much weaker than in the October 1989 flares. The precipitation sites were again located at the edges of sites of vertical currents, not within them, in contrast to sites of high coronal pressure. Figure 4 shows the flare of 20:35UT on 29 August 1990. The main site of non-thermal electron precipitation is located on the vertical field inversion line, to within our spatial resolution and co-registration accuracy, at the edge of a site of downward-directed vertical current. A second site, smaller and weaker, may be at the edge of a weak current or within it. Both the site of electron precipitation and the site of current are very small, and our resolution and co-registration uncertainty do not allow any meaningful statement. The site of highest coronal pressure (at about the time of Hα flare maximum) is located within a patch of downward vertical current.

5. Discussion

In all four observed flares in both active regions, the non-thermal electron precipitation sites were at the edges of the major vertical currents, whereas the sites of high coronal pressure were within them. To us, this suggests that acceleration occurs at sites of interaction of currents, and not at sites of current maxima. In contrast, in all four observed flares in both active regions the high-pressure sites were within patches of vertical current. Such high-pressure sites are doubtless the footpoints of the hottest, densest coronal flare structures, and would be the brightest features seen in X-rays had they been imaged during these events.

The combination of temporal development and morphology implies that these flares began at the edges of the current systems and spread toward their interiors. We attribute no particular significance to the presence of just one non-thermal precipitation site in the October flares. If one were to have very sensitive instrumentation, or even examine our October data with better sensitivity, we expect that the October flares might show more than one precipitation site. We also note that there is no single sign of the current at the dominant electron precipitation sites, implying that no simple model of enhanced resistivity in a region within the main current can explain the observational result.

We thank Bruce Lites for making available his least-squares Unno-fit Stokes profile code, Hal Zirin for BBSO images and videomagnetograms during October 1989 and Sandy McClymont and Yuhong Fan for help with many aspects of the analysis. This work has been supported by NASA grant NAGW 1542, NSF grant AST-8900716, and through Lockheed under NASA Contract NAS8-37344 with the NASA Marshall Space Flight Center.

References

Aly, J. J. 1989 *Solar Phys.* **120**, 19.

Canfield, R. C., Gunkler, T. A. & Ricchiazzi, P. J. 1984 *Astrophys. J.* **282**, 296.

Ding, Y. J., Hagyard, M. J., DeLoach, A. C., Hong, Q. F. & Liu, X. P. 1987 *Solar Phys.* **109**, 307.

Hagyard, M. J. 1988 *Solar Phys.* **115**, 1.

Lin, Y. & Gaizauskas, V. 1987 *Solar Phys.* **109**, 81.

Lites, B. W. & Skumanich, A. 1987 *Astrophys. J.* **322**, 473.

Mickey, D. L. 1975 *Solar Phys.* **97**, 223.

Moore, R. L., Hagyard, M. J. & Davis, J. M. 1987 *Solar Phys.* **113**, 347.

Moreton, G. E. & Severny, A. B. 1968 *Solar Phys.* **3**, 282.

Penn, M. J., Mickey, D. L., Canfield, R. C. & LaBonte, B. J. 1991 *Solar Phys.* (In the press.)

Sakurai, T., Makita, M. & Shibasaki, K. 1985 In *Theoretical problems in high-resolution solar physics* (MPA 212), p. 313. Max Planck Institute.

Discussion

E. R. Priest (*The University, St Andrews, U.K.*). (i) With your more robust magnetograms, do you agree with the Huntsville conditions for flare occurrence, namely that the shear exceed 80° or so along a length of polarity inversion line greater than 10 Mm or so? Are these conditions necessary and sufficient? (ii) At a similar meeting here 15 years ago, Cowling made the comment that it is more important to find the magnetic field than the electric current, since the latter is a secondary quantity which may be derived from the magnetic field. Because of the

PHILOSOPHICAL TRANSACTIONS OF THE ROYAL SOCIETY A MATHEMATICAL, PHYSICAL & ENGINEERING SCIENCES

resolution limits you are, of course, only finding the global currents. Your result that particles precipitate at the edge of a high-current region suggests possibly that it is occurring at the boundary between neighbouring interacting magnetic regions, one of which is more sheared than the other. However, there is more information in the magnetic field and so I would very much like to see you calculate the magnetic structures, their connectivity and the way they evolve during the flare.

R. C. Canfield. (i) We have not carried out an extensive study of the applicability of the conditions for flare occurrence identified by the Huntsville group. We have studied only three flares in one region and one flare in another. Nor are our magnetograms more robust for such a study, since the spatial resolution in the Huntsville data is significantly better than in ours, at least for the October 1989 region, and the azimuth of the magnetic field is not a difficult quantity to measure in either their magnetograms or ours, for fields of strength approaching 1000 Gauss. Nevertheless, upon casual examination, it appears that the conditions are met in all flares discussed in this paper. A much more complete study is necessary to establish whether the conditions are both necessary and sufficient. (ii) I would also like to see the development of robust techniques for calculation of magnetic structures in three dimensions in the corona above the photospheric plane in which the magnetic fields are measured. It would be very interesting to compare such coronal structures with those observed in the corona using the soft X-ray telescope aboard *Solar-A*. Of course, with the *Solar-A* SXT we will know more about the connectivity of such fields; without the coronal observations, and with our present poor capability to do field-line continuation, it is very much of a guessing game.

J. C. Hénoux (*Observatoire de Paris, France*). Lin & Gaizauskas (1987) pointed out a coincidence between the kernels of a flare, that occurred on 6 April 1980 in AR 2372, and the locations of the peak values in the electric current density. In cooperation with scientists from IAFE (Argentina) and MSFC (USA) we have computed, at the Paris Observatory, the shape and location of the separatrices in AR 2372. We found that (*a*) four out of five observed off-band Hα kernels were located on the separatrices, i.e. on the surfaces that separate cells of different connectivities; (*b*) there was a region close to the separator magnetically connected to the four kernels.

This gives strong support to a model where magnetic structures interact in the separator at the intersection of the separatrices and where the origin of the flare energy release is located on this separator. In AR 2372 no current is observed in the photospheric X points, indicating that the energy is not stored in a separator current but rather in currents flowing along the lines of force.

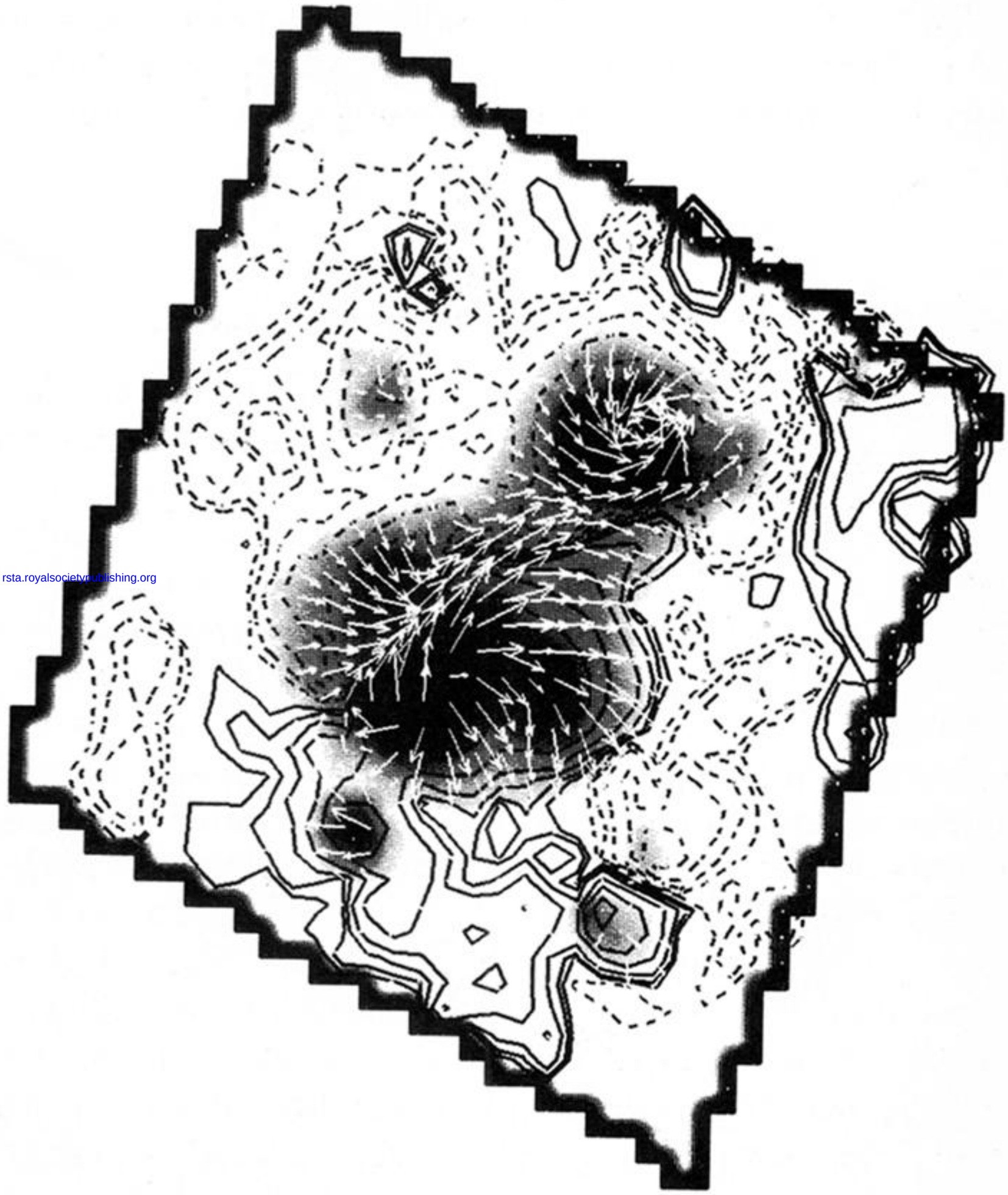

igure 1. The Mees Solar Observatory ambiguity-resolved vector magnetogram of 20 October 1989, canned from 17:41 to 18:33UT, transformed from image-plane to heliographic coordinates North is up, East to the left here and below). The gray-scale image shows the sunspot structure f the active region seen in the continuum near the $\lambda 6302.5$ line. The contours indicate the vertical agnetic field distribution averaged over each pixel. Radial field contours are shown at 25×2^n auss levels ($n = 0, 1, \ldots$; dashed contours indicate negative fields) here and below. The arrows ow the strength and direction of the transverse field; a length equal to the sampling interval presents a transverse field of strength *ca.* 700 gauss. (1 gauss $= 10^{-4}$ T.)

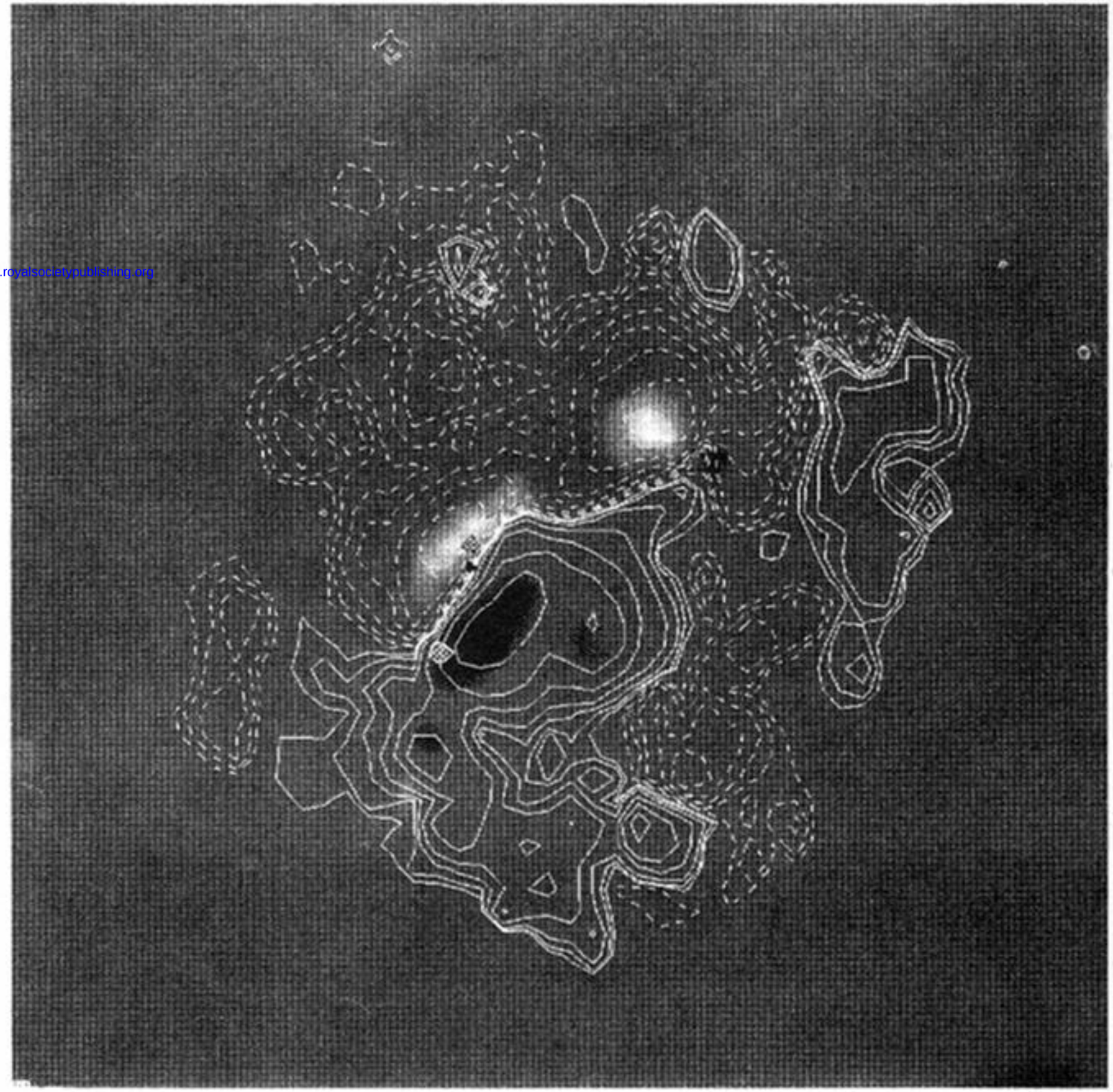

igure 3. Heliographic map of vertical current density (grey scale), vertical magnetic field ontours), and sites of the Hα signatures of non-thermal electron precipitation (solid black) and gh coronal pressure (cross-hatched black and white), in AR 5247 and the flare of 21:34UT on 20 ctober 1989. The image orientation and vertical field contours are the same as figure 1. Positive urrents are shown in white, negative in black. The terrestrial East–West dimension of the vector agnetogram is approximately 140 Mm.

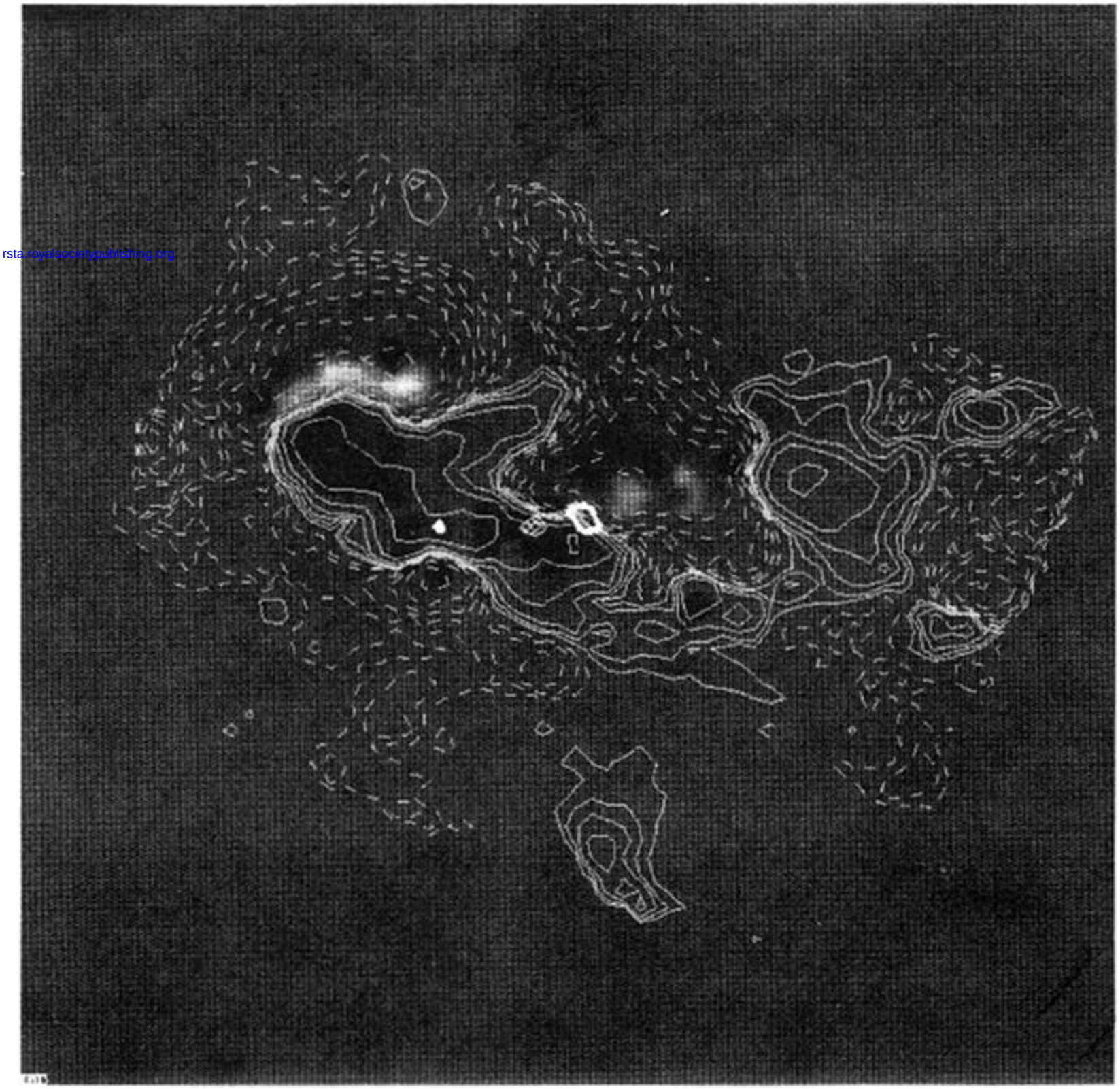

igure 4. Heliographic map of vertical current density (grey scale), vertical magnetic field ontours), and sites of the Hα signatures of non-thermal electron precipitation (white and white-ncircled) and high coronal pressure (white cross-hatched) in NOAA AR6233 and the flare of 0:35UT on 29 August 1990. The image orientation, current, and field conventions are the same s figure 3. The terrestrial East–West dimension of the magnetogram is approximately 114 Mm.